IEEE Access
Multidisciplinary | Rapid Review | Open Access Journal

SPECIAL SECTION ON ADVANCED MODELING AND CONTROL OF COMPLEX MECHATRONIC SYSTEMS WITH NONLINEARITY AND UNCERTAINTY

Received January 26, 2018, accepted February 25, 2018, date of publication March 8, 2018, date of current version April 23, 2018.

Digital Object Identifier 10.1109/ACCESS.2018.2813317

Nonlinear Motion Control of a Hydraulic Press Based on an Extended Disturbance Observer

CHUNGENG SUN, JINHUI FANG, JIANHUA WEI, AND BO HU
State Key Laboratory of Fluid Power and Mechatronic Systems, Zhejiang University, Hangzhou 310027, China

Corresponding author: Jinhui Fang (jhfang@zju.edu.cn)

This work was supported by the National Key Technology Research and Development Program of the Ministry of Science and Technology of China under Grant 2015BAF07B06.

ABSTRACT This paper focuses on high-performance motion control of the electro-hydraulic system of hydraulic presses. A detailed mathematical model of the system was constructed. An electro-hydraulic system of hydraulic presses is a kind of nonlinear system with parametric uncertainties, uncertain nonlinearities, and external disturbances. To attenuate the above effects, a nonlinear robust motion controller based on an extended disturbance observer was developed. The outer position tracking loop was designed with a sliding mode control to compensate for disturbance estimation error, while the inner pressure control loop using the backstepping method can realize accurate output force control. The stability of the overall closed-loop system based on the Lyapunov approach can be proven to be effective. Both simulation and experiment results showed that the proposed controller has a good transient-response and provides accurate position tracking in the presence of parametric uncertainties, uncertain nonlinearities, and external disturbances.

INDEX TERMS Hydraulic press, electro-hydraulic system, backstepping method, extended disturbance observer, motion control.

I. INTRODUCTION

Hydraulic presses are a kind of a machine tool and are widely used in various industries, such as the automobile, aerospace, and agricultural machinery industries. In a hydraulic press, force generation, transmission, and amplification are achieved using fluid under pressure. During the pressing and forming process, the hydraulic press needs to complete a process involving a cycle of acceleration, lowering in rapid traverse power, a working stoke, pressure holding, pressure relief, a slow return stroke, a fast return stroke, braking, and stop. In the process of a working stoke, it is necessary to track a predetermined trajectory [1], [2]. However, the electro-hydraulic system of hydraulic press is a nonlinear system and subjected to nonsmooth and discontinuous nonlinearities, such as a nonlinear pressure-flow relationship, directional change of valve opening, friction nonlinearity, and external disturbances. Furthermore, parametric uncertainties exist such as effective bulk modulus, leakage coefficient of the cylinder, and hydraulic oil density. The external load on an electro-hydraulic system of a hydraulic press also involves a large unknown parameter [3]. Despite the development of advanced control strategies in the last eight decades, the proportional-integral-derivative (PID) controller remains the most widely used control strategy in industry, because of its simplicity, robust performance and high reliability. A PID controller takes the current control error (P), past control error (I), and predicted future control error (D) into consideration; it acts like human's natural responses to outside stimulation [4], [5]. Until now, many advanced controllers have been proposed that achieved good control performance and can be compared with a classical PID controller. Strictly speaking, linear systems do not exist in practice, because all physical systems are nonlinear to some extent [6].

The dynamics of electro-hydraulic systems are highly nonlinear and are very sensitive to any change of in the PID parameters. When the controlled plant is complex, highly nonlinear, time-varying, and uncertain, it is necessary to adjust the PID parameters. To realize better dynamic performance, modeling uncertainties caused by parameter variations (e.g., bulk modulus and unknown load inertia) and external disturbances must be well-handled by the designed controller. Applying model-based advanced nonlinear control strategies to overcome the influence of parametric uncertainties, uncertain nonlinearities, and external disturbances in an electro-hydraulic system, is the current hot topic and development direction. The nonlinear problem of an electro-hydraulic system can be solved by nonlinear control strategies. Because an electro-hydraulic system is a kind of

semi-strict feedback nonlinear system, and parametric uncertainties and uncertain nonlinearities in the system are not directly related to the control law. That is, the model uncertainties of the system are not matched. This kind of system mainly uses a backstepping control approach to realize asymptotic stability [7]–[9]. The essence of backstepping is to stabilize the state of the virtual control, which can be derived by a Lyapunov function.

The effect of the external disturbances and uncertainties can be eliminated to improve the control accuracy of the system by applying an advanced control algorithm [10]. In order to obtain better tracking performance, a disturbance observer is an effective compensation method, because disturbances are not easy to measure in actual systems. In addition, a disturbance observer is widely used because of its simple structure, compensation for external disturbances, and model uncertainties [11]. External disturbances or unmodeled friction force will degrade position-tracking performance, because friction is an important source of nonlinearity in electro-hydraulic systems [12]. In the electro-hydraulic control, a high-pass disturbance observer was designed for position tracking and experimental results verified that the observer bandwidth could be cancelled. Kim *et al.* [13] proposed a two-order high pass filter to estimate disturbance which obtained good position tracking performance. Kim and Lee [14] estimated the torque disturbance of a variable displacement hydraulic motor and achieved good speed control. Wei *et al.* [15] designed a disturbance observer to estimate unknown time-varying load flow and achieved good supply pressure tracking performance. Model-based friction compensation can achieve accurate position control in machines with friction [16]. A variable structure system approach based was developed in designing observers for friction estimation and compensation in mechanical systems [17]. Han [5], [18] proposed an active disturbance rejection control, which proved to be a capable replacement of PID in practice. In a robotic manipulator control, several disturbance observers have been applied to estimate and compensate for unknown sources of disturbance [19], [20].

An exact mathematical model of the electro-hydraulic system is difficult to obtain because of the existing two types of uncertainties. One is parametric uncertainty, including bulk modulus, the square root relationship between pressure, and flow, temperature, and pressure dependent oil properties, the other is nonlinearity uncertainty, including friction and external disturbances [21], [22]. Yao *et al.* [23] proposed a practical nonlinear adaptive repetitive controller that would allow the model to learn and compensate for periodic modeling uncertainties with the goal of achieving asymptotic tracking performance. Yao [24] has developed adaptive robust control (ARC) theory, that when combined with both adaptive and robust control (such as sliding mode control), allows simultaneous solution systems with parametric uncertainties and uncertain nonlinearities. Guo *et al.* [25], [26] has proposed a saturated adaptive control to achieve tracking accuracy under unknown plant disturbance and parametric uncertainty. At present, ARC theory has been successfully applied to metal powder compaction presses [27], fast forging hydraulic presses [28], linear motor driven systems [29], [30], multilateral teleoperation systems, etc. [31]. Yao *et al.* [32] employed LuGre model-based friction compensation to achieve a high level tracking accuracy for hydraulic actuators. In addition, Sun *et al.* [33], [34] proposed a filter-based adaptive vibration control strategy for an electro-hydraulic active suspension to achieve closed-loop system performance and a novel model reference for adaptive control with an external filter to achieve better transient performance. Guo *et al.* [35] developed an extended disturbance observer to track the desired position trajectory for an electro-hydraulic system in the presence of both parametric uncertainties and external disturbance. Wei *et al.* [36] applied an extended fuzzy disturbance controller to the motion control of a fast forging hydraulic press and studied the low speed working systems under the action of an unknown load.

The rest of this paper is organized as follows. The second section describes problem formulation and dynamic models. The third section presents the proposed extended disturbance observer (EDO) controller design. The fourth section presents simulation setup and results. The fifth section presents experimental setup and results. The final section draws conclusions.

II. PROBLEM FORMULATION AND DYNAMIC MODELS

Hydraulic presses are suitable for a wide range of pressing, foaming, punching, and forming tasks. The electro-hydraulic system principle of the hydraulic press under consideration is depicted in Fig. 1. The nonlinear mathematical model of the hydraulic system was derived by theoretical analysis in the paper.

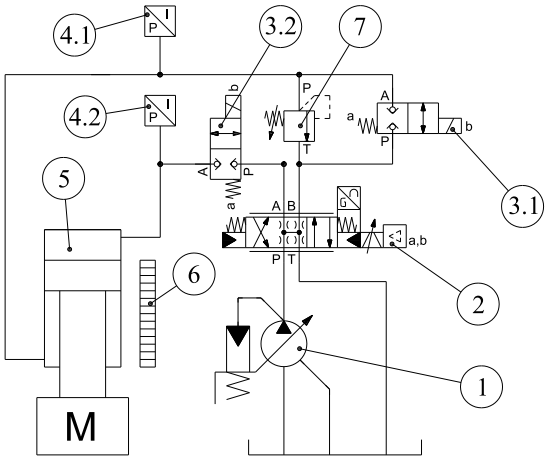

FIGURE 1. Schematic diagram of hydraulic system; 1–Constant pressure variable flow pump, 2–High-response servo proportional valve, 3–Solenoid 2/2 valve, 4–Pressure sensor, 5–Hydraulic cylinder, 6–Displacement sensor, 7–Relief valve.

The load force balance equation of the hydraulic cylinder can be described as (1)

$$m\ddot{x}_P = p_1A_1 - p_2A_2 - b\dot{x}_P - F_{co}\tanh(\dot{x}_P) + G - d \quad (1)$$

where m is the equivalent mass of the load, x_P is the displacement of the load, p_1 and p_2 are the pressure inside two chambers of the cylinder, A_1 and A_2 are the area inside two chambers of the cylinder, b is the combined coefficient of modelled damping and viscous friction forces on the load, F_{co} is the modelled coulomb friction force, G is the equivalent gravity of the load, and d is the lumped disturbance.

By neglecting both the internal and external leakage, the pressure dynamics can be expressed as (2)

$$\begin{aligned} \frac{V_{h1}}{\beta_e}\dot{p}_1 &= -A_1\dot{x}_P + Q_1 \\ \frac{V_{h2}}{\beta_e}\dot{p}_2 &= A_2\dot{x}_P - Q_2 \end{aligned} \tag{2}$$

The internal volume of the two chambers of the cylinder may be written as (3)

$$\begin{aligned} V_{h1} &= V_{01} + A_1 x_P \\ V_{h2} &= V_{02} + A_2 (L - x_P) \end{aligned} \tag{3}$$

where Q_1 and Q_2 are the flow through into the two chambers of the cylinder, V_{h1} and V_{h2} are the volume of the two chambers, V_{01} and V_{02} are the initial volume of the two chambers, β_e is the effective bulk modulus of the system, L is the hydraulic cylinder stroke.

The forward and return flow through the cylinder related to the high-response servo proportional valve (HSPV) described as:

$$\begin{cases} Q_1 = k_{qv}u\left[s_g(u)\sqrt{p_s - p_1} + s_g(-u)\sqrt{p_1 - p_t}\right] \\ Q_2 = k_{qv}u\left[s_g(u)\sqrt{p_2 - p_t} + s_g(-u)\sqrt{p_s - p_2}\right] \end{cases} \tag{4}$$

Now, by definition as:

$$s_g(\bullet) = \begin{cases} 1, & \text{if } \bullet \geq 0 \\ 0, & \text{if } \bullet < 0 \end{cases} \tag{5}$$

where k_{qv} is the HSPV flow gain coefficients, u is the HSPV control voltage, p_s is the pump supply pressure, and p_t is the tank pressure.

Define u as the control input and define the state variables x form as:

$x = [x_1, x_2, x_3, x_4]^T = [x_P, \dot{x}_P, p_1, p_2]^T$. The entire system, equations (1) to (4) can be expressed in the state space form

$$\begin{cases} \dot{x}_1 = x_2 \\ \dot{x}_2 = \dfrac{1}{m}\left[A_1x_3 - A_2x_4 - bx_2 - F_{co}\tanh(x_2) + G - d\right] \\ \dot{x}_3 = h_1\left(-A_1x_2 + k_{qv}g_3u\right) \\ \dot{x}_4 = h_2\left(A_2x_2 - k_{qv}g_4u\right) \end{cases} \tag{6}$$

in which

$$\begin{aligned} h_1 &= \frac{\beta_e}{V_{h1}} \\ h_2 &= \frac{\beta_e}{V_{h2}} \\ g_3 &= s_g(u)\sqrt{p_s - x_3} + s_g(-u)\sqrt{x_3 - p_t} \\ g_4 &= s_g(u)\sqrt{x_4 - p_t} + s_g(-u)\sqrt{p_s - x_4} \end{aligned} \tag{7}$$

III. CONTROLLER DESIGN

The extended disturbance observer is based on an extended state observer of $x_2$which is defined by:

$$\dot{\hat{x}}_{2p} = \frac{1}{m}\begin{bmatrix} A_1x_3 - A_2x_4 + G - F_{co}\tanh(x_2) \\ -\hat{b}x_2 - \hat{d} + w_1\tilde{x}_{2p} \end{bmatrix} \tag{8}$$

where $\hat{x}_{2p}$, $\hat{b}$ and $\hat{d}$ are the estimations of x_2, b and d, respectively.

$$\begin{aligned} \tilde{b} &= b - \hat{b} \\ \tilde{d} &= d - \hat{d} \\ \tilde{x}_{2p} &= x_2 - \hat{x}_{2p} \end{aligned} \tag{9}$$

In (9), $\hat{\bullet}$ represents the estimation of the parameter, $\tilde{\bullet}$ represents the estimation error of the parameter, and is defined as $\tilde{\bullet} = \hat{\bullet} - \bullet$. The dynamics of $\tilde{x}_{2p}$ may be obtained as follows:

$$\dot{\tilde{x}}_{2p} = -\frac{1}{m}\left(\tilde{b}x_2 + \tilde{d} + w_1\tilde{x}_{2p}\right) \tag{10}$$

The adaptation law is designed as follows:

$$\begin{aligned} \dot{\hat{b}} &= -k_{11}\frac{1}{m}x_2\tilde{x}_{2p} + \chi_b \\ \dot{\hat{d}} &= \mathrm{Proj}_{\hat{d}}\left(-k_{12}\frac{1}{m}\tilde{x}_{2p}\right) \end{aligned} \tag{11}$$

where k_{11} and k_{12} are positive constants, χ_b is an extra corrector term designed to ensure the stabilizing effect of the closed-loop system which will be specified later.

The simple discontinuous projection mapping has the form as

$$\mathrm{Proj}_{\hat{d}}(\bullet) = \begin{cases} 0, & \hat{d} = \hat{d}_{\max} \;\&\; \bullet > 0 \\ 0, & \hat{d} = \hat{d}_{\min} \;\&\; \bullet < 0 \\ \bullet, & \text{otherwise} \end{cases} \tag{12}$$

The conditions that are used in (12) to guarantees

$$\begin{cases} I. \quad d_{\min} \leq \hat{d} \leq d_{\max} \\ II. \quad \tilde{d}\left[-\dfrac{1}{m}\tilde{x}_{2p} - k_{12}^{-1}\dot{\hat{d}}\right] \leq 0 \end{cases} \tag{13}$$

Define a positive semi-definite function

$$V_1 = \frac{1}{2}\tilde{x}_{2p}^2 + \frac{1}{2}k_{11}^{-1}\tilde{b}^2 + \frac{1}{2}k_{12}^{-1}\tilde{d}^2 \tag{14}$$

From (9), we can deduct

$$\begin{aligned} \dot{\tilde{b}} &= -\dot{\hat{b}} \\ \dot{\tilde{d}} &= -\dot{\hat{d}} \end{aligned} \tag{15}$$

Noting (15), the time derivative of (14) is given by

$$\dot{V}_1 = -\frac{1}{m}w_1\tilde{x}_{2p}^2 + \tilde{d}\left(-\frac{1}{m}\tilde{x}_{2p} - k_{12}^{-1}\dot{\hat{d}}\right) - k_{11}^{-1}\tilde{b}\chi_b \tag{16}$$

Define the motion trajectory tracking error of the cylinder

$$z_1 = x_1 - x_{1d} \tag{17}$$

where x_{1d} is the desired trajectory of the cylinder.

A sliding surface s is defined as follows:

$$s = \dot{z}_1 + \lambda z_1 \tag{18}$$

where λ is a positive constant.

Since $G(s) = 1/(s+\lambda)$ is a stable transfer function, making z_1 small or converging to zero, this is equivalent to making s small or converging to zero.

The time derivative of (18) and noting (6), it is straightforward to obtain

$$\dot{s} = \frac{1}{m}\left[A_1 x_3 - A_2 x_4 + G - F_{co}\tanh(x_2) - bx_2 - d\right] - \ddot{x}_{1d} + \lambda(x_2 - \dot{x}_{1d}) \tag{19}$$

Let $p_L = A_1 x_3 - A_2 x_4$ denotes the virtual control input and let $z_2 = p_L - \alpha_2$ denotes the input discrepancy. In view of p_L, the desired virtual control function α_2 is designed as equation (20)

$$\alpha_2 = -G + F_{co}\tanh(x_2) + \hat{b}x_2 + \hat{d} + m\left[\ddot{x}_{1d} - \lambda(x_2 - \dot{x}_{1d}) - c_1 s - c_2 sgn(s)\right] \tag{20}$$

where c_1 and c_2 are both positive constants.

The term $-c_2 sgn(s)$ is designed to compensate for disturbance estimation errors and c_2 is given to satisfy

$$c_2 > \left|\tilde{d}\right|_{\max}/m \tag{21}$$

Noting (20) and (19), one obtains

$$\dot{s} = -c_1 s - c_2 sgn(s) + \frac{1}{m}z_2 - \frac{1}{m}\tilde{b}x_2 - \frac{\tilde{d}}{m} \tag{22}$$

Define a positive semi-definite function

$$V_2 = V_1 + \frac{1}{2}k_2^{-1}s^2 \tag{23}$$

where k_2 is a positive constant.

Noting (16) and (22), the time derivative of (23) is given by

$$\dot{V}_2 = -\frac{1}{m}w_1\tilde{x}_{2p}^2 + \tilde{d}\left(-\frac{1}{m}\tilde{x}_{2p} - k_{12}^{-1}\dot{\hat{d}}\right) - k_{11}^{-1}\tilde{b}\chi_b + k_2^{-1}\left(-c_1 s^2 - c_2|s| - \frac{1}{m}\tilde{d}s + \frac{1}{m}z_2 s - \frac{1}{m}x_2\tilde{b}s\right) \tag{24}$$

The extra corrector term χ_b was chosen as:

$$\chi_b = -k_{11}k_2^{-1}\frac{1}{m}x_2 s \tag{25}$$

Substituting (25) into (24) yields

$$\dot{V}_2 = -\frac{1}{m}w_1\tilde{x}_{2p}^2 - c_1 k_2^{-1}s^2 + \tilde{d}\left(-\frac{1}{m}\tilde{x}_{2p} - k_{12}^{-1}\dot{\hat{d}}\right) + k_2^{-1}\left(-c_2|s| - \frac{1}{m}\tilde{d}s\right) + k_2^{-1}\frac{1}{m}z_2 s \tag{26}$$

Differentiating p_L with respect to time yields

$$\dot{p}_L = A_1\dot{x}_3 - A_2\dot{x}_4 \tag{27}$$

Substituting (6) into (27), $\dot{p}_L$ can be obtained

$$\dot{p}_L = -\left[A_1^2 h_1 + A_2^2 h_2\right]x_2 + k_{qv}\left[A_1 h_1(x_1)ug_3 + A_2 h_2(x_1)ug_4\right] \tag{28}$$

Defining

$$\begin{aligned} f_1(x_1) &= A_1^2 h_1 + A_2^2 h_2 \\ f_2(x_1, x_3, x_4, u) &= A_1 h_1 g_3 + A_2 h_2 g_4 \end{aligned} \tag{29}$$

Substituting (29) into (28) yields

$$\dot{p}_L = -f_1 x_2 + k_{qv} f_2 u \tag{30}$$

According to the virtual control input $z_2 = p_L - \alpha_2$, one obtains

$$p_L = z_2 + \alpha_2 \tag{31}$$

Substituting (31) into (30) yields

$$\dot{z}_2 = -f_1 x_2 + k_{qv} f_2 u - \dot{\alpha}_2 \tag{32}$$

The following control law u is designed as

$$u = \frac{1}{k_{qv} f_2}\left(f_1 x_2 + \dot{\alpha}_2 - c_3 z_2 - k_2^{-1}k_{31}\frac{1}{m}s\right) \tag{33}$$

where c_3 and k_{31} are positive constants. Substituting (33) into (32), the dynamics of z_2 can be obtained

$$\dot{z}_2 = -c_3 z_2 - k_2^{-1}k_{31}\frac{1}{m}s \tag{34}$$

Define a positive semi-definite function

$$V = V_2 + \frac{1}{2}k_{31}^{-1}z_2^2 \tag{35}$$

Noting (26) and (34), the time derivative of (35) is given by

$$\dot{V} = -\frac{1}{m}w_1\tilde{x}_{2p}^2 - c_1 k_2^{-1}s^2 - c_3 k_{31}^{-1}z_2^2 < 0 \tag{36}$$

Equation (36) indicates that the stability of the closed-loop system consisting of the nonlinear controller; the EDO was guaranteed. Furthermore, all signals in the system were bounded under closed-loop operation.

IV. SIMULATION SETUP AND RESULTS

A. SIMULATION SETUP

To validate the performance of the proposed EDO controller, simulations based on MATLAB/AMESim co-simulation platform were performed. A co-simulation model of hydraulic press electro-hydraulic system was plotted under the gravitation conditions in Fig. 2. In order to shorten the length of this paper, the co-simulation model was not plotted under external load conditions. The model under external load conditions can refer to the schematic diagram of the hydraulic system (Fig. 1). The pressure setting of the relief valve was 14MPa; the working stoke stage of the hydraulic press could be simulated.

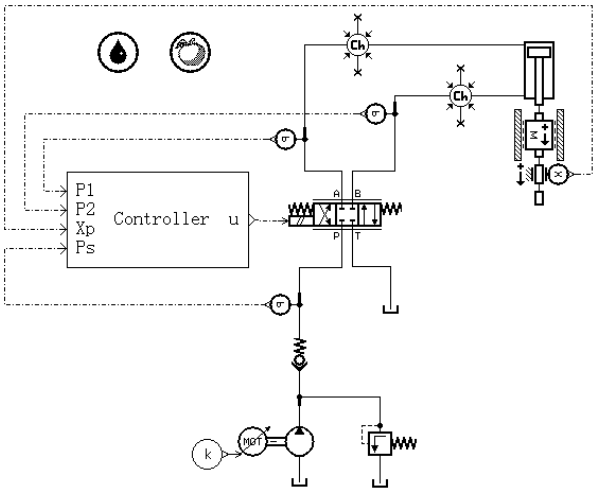

FIGURE 2. Simulation model of electro-hydraulic system.

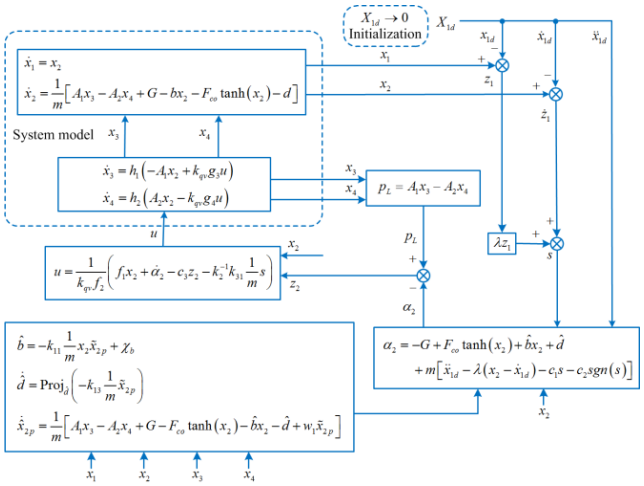

FIGURE 3. Principle diagram of the extended disturbance observer.

TABLE 1. Values of electro-hydraulic system.

Parameter(unit)	Value	Parameter(unit)	Value
$M/(kg)$	175.0	$L/(m)$	0.21
$A_1/(m^2)$	5.0265	$A_2/(m^2)$	3.0361
$p_s/(p_a)$	2.0×10^{7}	$p_t/(p_a)$	0
$F_{co}/(N)$	1.2×10^{3}	$b/(N\cdot s/m)$	1.0×10^{5}
$V_{01}/(m^3)$	3.0877×10^{-4}	$V_{02}/(m^3)$	2.3529×10^{-4}
$k_{qv}/(m^3/sV\sqrt{p_a})$	3.5635×10^{-8}		

The structure of the EDO controller is illustrated in Fig. 3. The parameters of the electro-hydraulic system in simulations and the EDO controller are given in Tables 1 and 2, respectively.

The simulation performance of the proposed EDO controller was compared with that of the ARC [22] and PID controllers. The desired displacement signals of trajectory I and II are shown in (37) and (38), respectively

$$x_d^I = \left[60\sin\left(\frac{\pi}{6}t+\frac{\pi}{2}\right)+60\right]\text{mm}, \quad 0\le t\le 120 \tag{37}$$

$$x_d^{II} = \left[60\sin\left(\frac{\pi}{6}t+\frac{\pi}{2}\right)+60\right]\text{mm}, \quad 0\le t\le 6 \tag{38}$$

TABLE 2. Values of the extended disturbance observer in the simulation.

Parameter	Value	Parameter	Value
w_1	6.0×10^{3}	k_2	1.0×10^{2}
λ	60.0	k_3	5.0
k_{11}	5.0×10^{5}	c_1	20.0
k_{12}	8.0	c_2	10.0
k_{31}	1.0	c_3	1.5×10^{2}
$\hat{b}(0)$	1.0×10^{5}	$\hat{d}(0)$	0

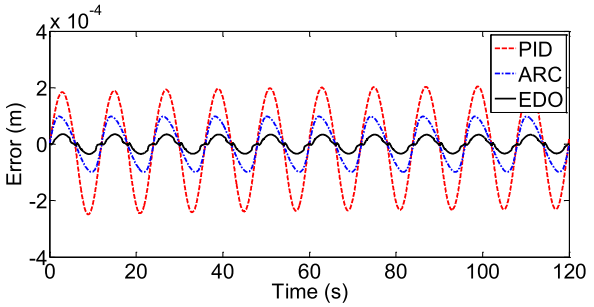

FIGURE 4. Positioning errors of trajectory I in the simulation.

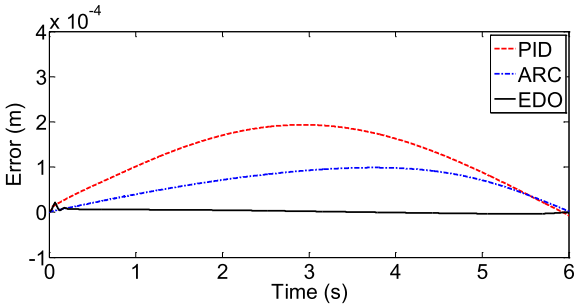

FIGURE 5. Positioning errors of trajectory II in the simulation.

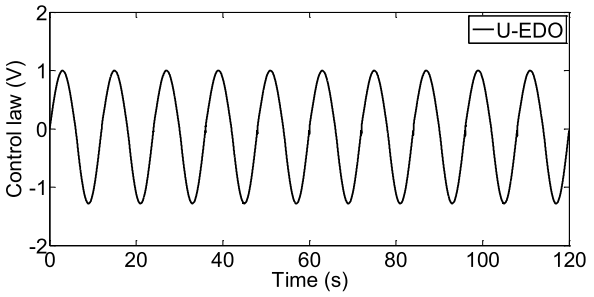

FIGURE 6. Control law of trajectory I in the simulation.

The PID controller parameters of trajectories I and II were tuned to the values that guaranteed the best tracking performance in the simulations and the experiments; these are shown in (39) and (40)

$$u_{PID}^S = 2300\,(x_{1d}-x_1)+100\int_0^t (x_{1d}-x_1)dt + 10\,(\dot{x}_{1d}-\dot{x}_1) \tag{39}$$

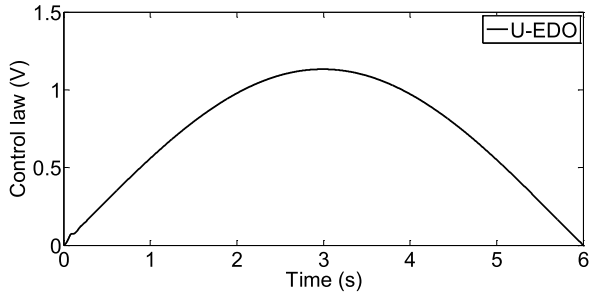

FIGURE 7. Control law of trajectory II in the simulation.

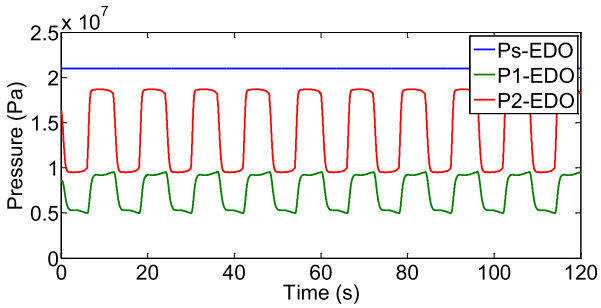

FIGURE 8. Pressures of trajectory I in the simulation.

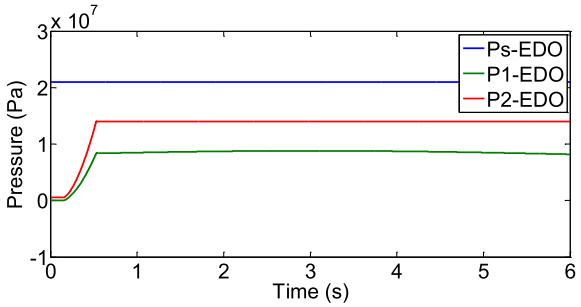

FIGURE 9. Pressures of trajectory II in the simulation.

$$u_{PID}^{E} = 1800\,(x_{1d} - x_1) + 300\int_0^t (x_{1d} - x_1)dt + 10\,(\dot{x}_{1d} - \dot{x}_1) \tag{40}$$

B. SIMULATION RESULTS

The position tracking errors of trajectories I and II are shown in Figs. 4 and 5, respectively. The tracking error of the proposed EDO controller with trajectory I was kept within $\pm 5 \times 10^{-5}$ m, while the tracking errors of the ARC and PID controllers were kept within $\pm 1 \times 10^{-4}$ m and $\pm 2 \times 10^{-4}$ m, respectively (Fig. 4). The tracking error of the proposed EDO controller with trajectory II was kept within $\pm 2 \times 10^{-5}$ m, while the tracking errors of the ARC and PID controllers were kept respectively within $\pm 1 \times 10^{-4}$ m and $\pm 2 \times 10^{-4}$ m (Fig. 5). The control laws of the proposed EDO controller with trajectories I and II are shown in Figs. 6 and 7, respectively. The pressures p_s, $p_1$and p_2 are shown in Figs. 8 and 9, respectively. The parameter estimations of the EDO are shown in Figs. 10 and 11, respectively.

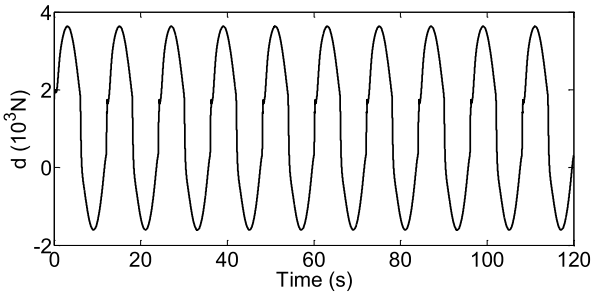

FIGURE 10. Parameter estimation of trajectory I in the simulation.

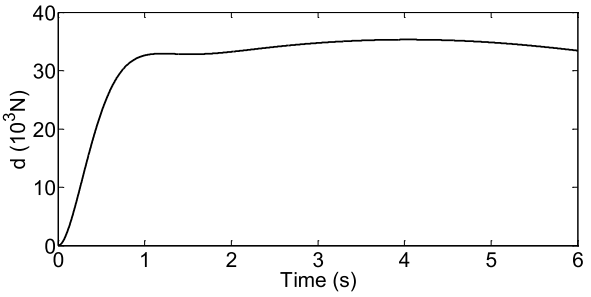

FIGURE 11. Parameter estimation of trajectory II in the simulation.

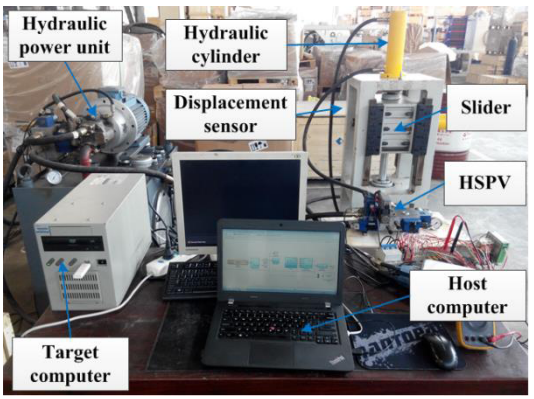

FIGURE 12. Photograph of experimental setup.

V. EXPERIMENTAL SETUP AND RESULTS

A. EXPERIMENTAL SETUP

A photograph of the experimental setup is shown in Fig. 12. The system using a hydraulic press was mainly composed of a frame, a cylinder, an HSPV, and a slider. In the test rig, the driving actuator was controlled by a HSPV (REXROTH: 4WRREH6VB40L-1X/G24K0/B5M), which had a bandwidth above 80 Hz with a $\pm$ 100% control signal. The system state variables used in the controller, including actuator's displacement x_1 and velocity x_2, that is, the differential of displacenment, and pressures in the two working chambers x_3 and x_4 were directly measured by transducers (WIKA: S10/0-250BAR/4-20MA/G1/4A) which had a range of 0–25 MPa. The supply pressure p_s was regulated to 20 MPa. The displacement of the actuator was directly obtained by a position tranducer (SMAT: MS200-30+MR200c-3). The control strategy was carried out in the xPC Target environment, which consisted of a target computer equipped with an

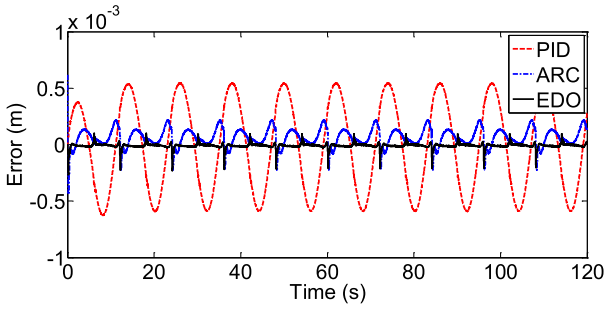

FIGURE 13. Positioning errors of trajectory I in the experiment.

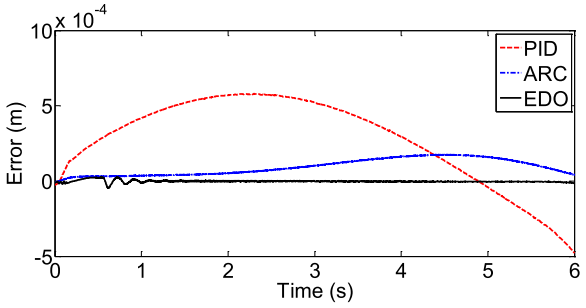

FIGURE 14. Positioning errors of trajectory II in the experiment.

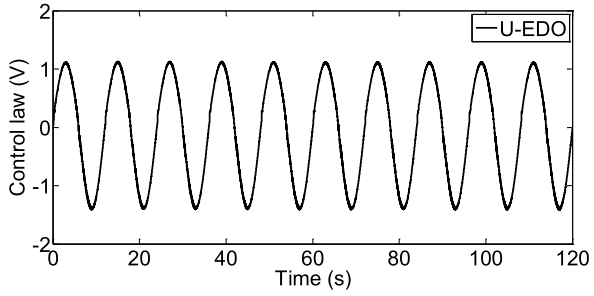

FIGURE 15. Control law of trajectory I in the experiment.

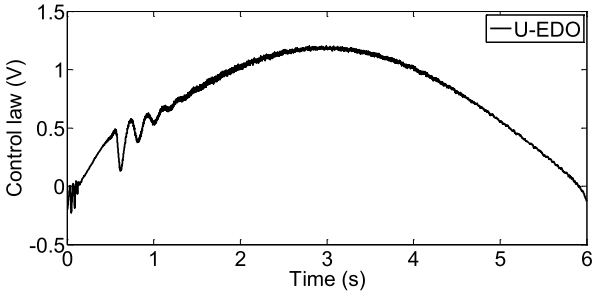

FIGURE 16. Control law of trajectory II in the experiment.

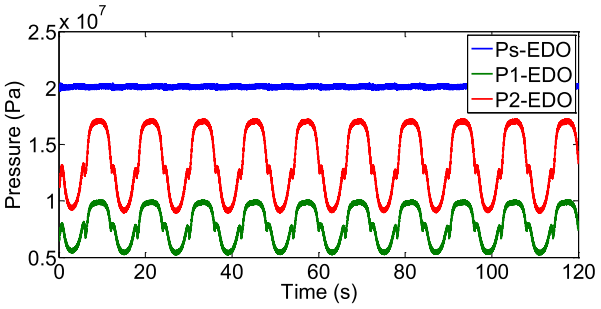

FIGURE 17. Pressures of trajectory I in the experiment.

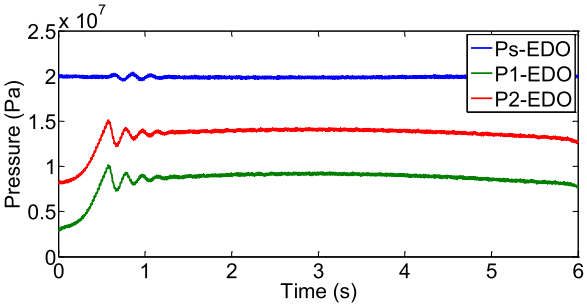

FIGURE 18. Pressures of trajectory II in the experiment.

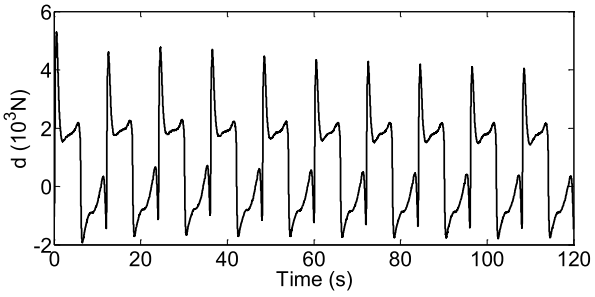

FIGURE 19. Parameter estimation of trajectory I in the experiment.

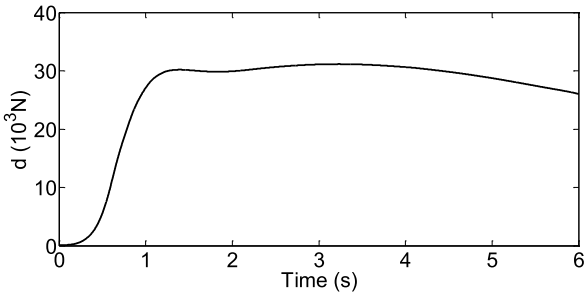

FIGURE 20. Parameter estimation of trajectory II in the experiment.

NI PCI-6259 data acquisition board manufactured by NI Corp. (Austin, TX, USA) and a host computer with MATLAB/Simulink. All the measurement signals were fed back to the controller using 16 bit A/D and 16 bit D/A converters. Data transmission between the target and the computers was achieved through TCP/IP. The controller sampling rate was 1 KHz. The parameters of the EDO controller in the experiments are given in Table 3.

B. EXPERIMENTAL RESULTS

The position tracking errors of trajectories I and II are shown in Figs. 13 and 14, respectively. The tracking error of the proposed EDO controller with trajectory I was kept within $\pm 2 \times 10^{-4}$ m, while the tracking errors of the ARC and PID controllers were kept within $\pm 2.5 \times 10^{-4}$ m and $\pm 6 \times 10^{-4}$ m, respectively (Fig. 13). The tracking error of the proposed EDO controller with trajectory II was kept

TABLE 3. Values of extended disturbance observer in the experiment.

Parameter	Value	Parameter	Value
w_1	8.0×10^{3}	k_2	1.0×10^{2}
λ	80.0	k_3	5.0
k_{11}	5.0×10^{5}	c_1	20.0
k_{12}	8.0	c_2	10.0
k_{31}	1.0	c_3	1.5×10^{2}
$\hat{b}(0)$	1.0×10^{5}	$\hat{d}(0)$	0

within $\pm1 \times 10^{-4}$ m, while the tracking errors of the ARC and PID controllers were kept within $\pm2 \times 10^{-4}$ m and $\pm6 \times 10^{-4}$ m, respectively (Fig. 14). The control laws of the proposed EDO controller with trajectories I and II are shown in Figs. 15 and 16, respectively. The pressures p_s, p_1 and p_2 are shown in Figs. 17 and 18, respectively. The parameter estimations of the EDO are shown in Figs. 19 and 20, respectively.

VI. CONCLUSION

A nonlinear motion controller based on an extended disturbance observer was designed with a detailed mathematical model of an elecrtro-hydraulic system using a hydraulic press. The controller was made of a dual control loop comprised of an inner pressure control loop and an outer position tracking loop. The stability of the overall closed-loop system was guaranteed by the Lyapunov theory. Simulations and experiments showed that good control performance was achieved and the proposed controller guaranteed position tracking accuracy for tracking both trajectories I and II, when compared with two other controllers.

REFERENCES

[1] H.-X. Li and X. Lu, *System Design and Control Integration for Advanced Manufacturing*. Hoboken, NJ, USA: Wiley, 2014.

[2] M. Yuan, Z. Chen, B. Yao, and X. Zhu, "Time optimal contouring control of industrial biaxial gantry: A highly efficient analytical solution of trajectory planning," *IEEE/ASME Trans. Mechatronics*, vol. 22, no. 1, pp. 247–257, Feb. 2017.

[3] H. E. Merritt, *Hydraulic Control Systems*. New York, NY, USA: Wiley, 1967.

[4] K. J. Åström and T. Hägglund, "The future of PID control," *Control Eng. Pract.*, vol. 9, no. 11, pp. 1163–1175, Apr. 2001.

[5] J. Han, "From PID to active disturbance rejection control," *IEEE Trans. Ind. Electron.*, vol. 56, no. 3, pp. 900–906, Mar. 2009.

[6] B. Yao and C. Jiang, "Advanced motion control: From classical PID to nonlinear adaptive robust control," in *Proc. 11th IEEE Int. Workshop Adv. Motion Control*, Niigata, Japan, Mar. 2010, pp. 815–829.

[7] A. Alleyne and R. Liu, "A simplified approach to force control for electro-hydraulic systems," *Control Eng. Pract.*, vol. 8, no. 12, pp. 1347–1356, Deb. 2000.

[8] C. Kaddissi, J.-P. Kenné, and M. Saad, "Indirect adaptive control of an electrohydraulic servo system based on nonlinear backstepping," *IEEE/ASME Trans. Mechatronics*, vol. 16, no. 6, pp. 1171–1177, Dec. 2011.

[9] W. Kim, D. Won, D. Shin, and C. C. Chung, "Output feedback nonlinear control for electro-hydraulic systems," *Mechatronics*, vol. 22, no. 6, pp. 766–777, 2012.

[10] Q. Guo and D. Jiang, *Nonlinear Control Techniques for Electro-Hydraulic Actuators in Robotics Engineering*. Boca Raton, FL, USA: CRC Press, 2017.

[11] S. Li, J. Yang, W.-H. Chen, and X. Chen, *Disturbance Observer-Based Control: Methods and Applications*. Boca Raton, FL, USA: CRC Press, 2014.

[12] A. Bonchis, P. I. Corke, D. C. Rye, and Q. P. Ha, "Variable structure methods in hydraulic servo systems control," *Automatica*, vol. 37, no. 4, pp. 589–595, Apr. 2001.

[13] W. Kim, D. Shin, D. Won, and C. C. Chung, "Disturbance-observer-based position tracking controller in the presence of biased sinusoidal disturbance for electrohydraulic actuators," *IEEE Trans. Control Syst. Technol.*, vol. 21, no. 6, pp. 2290–2298, Nov. 2013.

[14] C.-S. Kim and C.-O. Lee, "Speed control of an overcentered variable-displacement hydraulic motor with a load-torque observer," *Control Eng. Pract.*, vol. 4, no. 4, pp. 1563–1570, Nov. 1996.

[15] J. Wei, K. Guo, J. Fang, and Q. Tian, "Nonlinear supply pressure control for a variable displacement axial piston pump," *Proc. Inst. Mech. Eng. I, J. Mech. Eng. Sci.*, vol. 229, no. 7, pp. 614–624, Apr. 2015.

[16] B. Armstrong-Hélouvry, P. Dupont, and C. C. De Wit, "A survey of models, analysis tools and compensation methods for the control of machines with friction," *Automatica*, vol. 30, pp. 1083–1138, Jul. 1994.

[17] Q. P. Ha, A. Bonchis, D. C. Rye, and H. F. Durrant-Whyte, "Variable structure systems approach to friction estimation and compensation," in *Proc. IEEE Int. Conf. Robot. Autom.*, Apr. 2000, pp. 3543–3548.

[18] J.-Q. Han, "Nonlinear design methods for control systems," in *Proc. 14th IFAC World Congr.*, Beijing, China, 1999, pp. 521–526.

[19] S. P. Chan, "A disturbance observer for robot manipulators with application to electronic components assembly," *IEEE Trans. Ind. Electron.*, vol. 42, no. 5, pp. 487–493, Oct. 1995.

[20] B. K. Kim, W. K. Chung, and Y. Youm, "Robust learning control for robot manipulators based on disturbance observer," in *Proc. IEEE Ind. Electron. Conf.*, Aug. 1996, pp. 1276–1282.

[21] B. Yao, F. Bu, and G. T. C. Chiu, "Non-linear adaptive robust control of electro-hydraulic systems driven by double-rod actuators," *Int. J. Control*, vol. 74, no. 8, pp. 761–775, 2001.

[22] B. Yao, F. Bu, J. Reedy, and G. T.-C. Chiu, "Adaptive robust motion control of single-rod hydraulic actuators: Theory and experiments," *IEEE/ASME Trans. Mechatronics*, vol. 5, no. 1, pp. 79–91, Mar. 2000.

[23] J. Yao, Z. Jiao, and D. Ma, "A practical nonlinear adaptive control of hydraulic servomechanisms with periodic-like disturbances," *IEEE/ASME Trans. Mechatronics*, vol. 20, no. 6, pp. 2752–2760, Dec. 2015.

[24] B. Yao, "High performance adaptive robust control of nonlinear systems: A general framework and new schemes," in *Proc. IEEE Conf. Decision Control*, Dec. 1997, pp. 2489–2494.

[25] Q. Guo, J. Yin, T. Yu, and D. Jiang, "Saturated adaptive control of an electrohydraulic actuator with parametric uncertainty and load disturbance," *IEEE Trans. Ind. Electron.*, vol. 64, no. 10, pp. 7930–7941, Oct. 2017.

[26] Q. Guo, Y. Zhang, B. G. Celler, and S. W. Su, "Backstepping control of electro-hydraulic system based on extended-state-observer with plant dynamics largely unknown," *IEEE Trans. Ind. Electron.*, vol. 63, no. 11, pp. 6909–6920, Nov. 2016.

[27] R.-L Feng and J. Wei, "Adaptive robust motion control of powder compaction press," *Trans. Chin. Soc. Agric. Mach.*, vol. 46, no. 8, pp. 352–360 and 337, 2015.

[28] Q. Zhang, J. Fang, J. Wei, Y. Xiong, and G. Wang, "Adaptive robust motion control of a fast forging hydraulic press considering the nonlinear uncertain accumulator model," *Proc. Inst. Mech. Eng. I, J. Syst. Control Eng.*, vol. 230, no. 6, pp. 483–497, Feb. 2016.

[29] Z. Chen, B. Yao, and Q. Wang, "Accurate motion control of linear motors with adaptive robust compensation of nonlinear electromagnetic field effect," *IEEE/ASME Trans. Mechatronics*, vol. 18, no. 3, pp. 1122–1129, Jun. 2013.

[30] Z. Chen, B. Yao, and Q. Wang, "μ-synthesis-based adaptive robust control of linear motor driven stages with high-frequency dynamics: A case study," *IEEE/ASME Trans. Mechatronics*, vol. 20, no. 3, pp. 1482–1490, Jun. 2015.

[31] Z. Chen, Y.-J. Pan, and J. Gu, "Integrated adaptive robust control for multilateral teleoperation systems under arbitrary time delays," *Int. J. Robust Nonlinear Control*, vol. 26, no. 12, pp. 2708–2728, Aug. 2016.

[32] J. Yao, W. Deng, and Z. Jiao, "Adaptive control of hydraulic actuators with LuGre model-based friction compensation," *IEEE Trans. Ind. Electron.*, vol. 62, no. 10, pp. 6469–6477, Oct. 2015.

[33] W. Sun, H. Pan, and H. Gao, "Filter-based adaptive vibration control for active vehicle suspensions with electrohydraulic actuators," *IEEE Trans. Veh. Technol.*, vol. 65, no. 6, pp. 4619–4626, May 2016.

[34] W. Sun, Y. Zhang, Y. Huang, H. Gao, and O. Kaynak, "Transient-performance-guaranteed robust adaptive control and its application to precision motion control systems," *IEEE Trans. Ind. Electron.*, vol. 63, no. 10, pp. 6510–6518, Mar. 2016.
[35] K. Guo, J. Wei, and Q. Tian, "Nonlinear adaptive position tracking of an electro-hydraulic actuator," *Proc. Inst. Mech. Eng. C, J. Mech. Eng. Sci.*, vol. 229, no. 17, pp. 3252–3265, 2015.
[36] J. Wei, Q. Zhang, M. Li, and W. Shi, "High-performance motion control of the hydraulic press based on an extended fuzzy disturbance observer," *Proc. Inst. Mech. Eng. I, J. Syst. Control Eng.*, vol. 230, no. 9, pp. 1044–1061, Aug. 2016.

CHUNGENG SUN received the M.S. degree in mechatronic control engineering from the Kunming University of Science and Technology, Kunming, China. He is currently pursuing the Ph.D. degree in mechatronic control engineering with Zhejiang University, Hangzhou, China. He has taken part in several applications and research projects from electro-hydraulic control system in various organizations. His research interests include the hydraulic presses, advanced motion control of electro-hydraulic systems, synchronization control, and industry automation.

JINHUI FANG received the Ph.D. degree in fluid power transmission and control from Zhejiang University, Hangzhou, China, in 2013. He is currently an Assistant Research Fellow with the State Key Laboratory of Fluid Power Transmission and Control, Zhejiang University. His current research interests include the modeling and control of hydraulic components and electro-hydraulic systems, the sliding-mode control, and other nonlinear control in fluid power.

JIANHUA WEI received the Ph.D. degree in fluid power transmission and control from Zhejiang University, Hangzhou, China, in 1995. He is currently a Professor with the State Key Laboratory of Fluid Power and Mechatronic Systems, Zhejiang University. His current research interests include actuators, fluid power, and transmission.

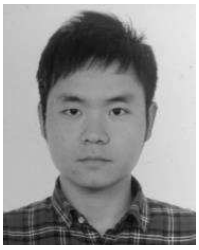

BO HU received the B.Eng. degree from Zhejiang University, Hangzhou, China, in 2010. He is currently pursuing the Ph.D. degree with the State Key Laboratory of Fluid Power and Mechatronic Systems, Zhejiang University, Hangzhou, China. His research focuses on design, modeling, identification, and control of electro-hydraulic systems in construction machine.